Powder Technology 209 (2011) 119–123

Contents lists available at ScienceDirect

Powder Technology

journal homepage: www.elsevier.com/locate/powtec

Effect of Fe(II) on the formation of iron oxide synthesized from pyrite cinders by hydrothermal process

Zhaocheng Liu, Yajie Zheng *

School of Metallurgical Science and Engineering, Central South University, Changsha 410083, PR China

A R T I C L E I N F O

Article history:
Received 15 September 2010
Received in revised form 12 February 2011
Accepted 17 February 2011
Available online 23 February 2011

Keywords:
Hydrothermal process
Iron oxide
Pyrite cinders
Fe(II)
Formation mechanism

A B S T R A C T

The effect of Fe(II) on the formation of iron oxide particles, synthesized from pyrite cinders lixivium via hydrothermal process, is investigated using X-ray diffraction (XRD), Fourier transform infrared spectroscopy (FT-IR), scanning electron microscope (SEM), transmission electron microscopy (TEM) and selected area electron diffraction (SAED). The results indicate that Fe(II) can significantly affect the formation of iron oxide particles and the properties of the synthesized iron oxide particles. When $n_{Fe(II)}/n_{Fe(III)}$ varies from 0 to 0.1, all the samples are crystallized to hematite (α-Fe_2O_3), without any other phase. Particle size of the prepared hematite gradually increases with the increase of $n_{Fe(II)}/n_{Fe(III)}$ ratio, while the shape of the prepared hematite changes from sphere into platelet. When the $n_{Fe(II)}/n_{Fe(III)}$ increases to 0.12, both α-Fe_2O_3 and Fe_3O_4 are formed and the shape of the product becomes spherical. As for the formation mechanism, it is found that Fe(II) can accelerate the phase transformation. The transformation process without Fe(II) is dissolution re-precipitation. However, in the transformation process with trace Fe(II), the phase transformation is dominated by solid-state transformation, though dissolution re-precipitation is still function. In addition, the formation of platelet-type hematite particles is attributed to that Al^{3+} ions are adsorbed onto {0001} face.

1. Introduction

Pyrite cinders are produced as a by-product of sulfuric acid industry. In China, more than 30% sulfuric acid is produced from pyrites. However, to obtain 1 t sulfuric acid, 0.7–1.0 t pyrite cinders will be generated, depending on the scale of sulfuric acid production plants. Therefore, over 10 million tons of pyrite cinders are generated annually in China. Pyrite cinders are mainly composed by iron oxides in the form of hematite (Fe_2O_3) and magnetite (Fe_3O_4). And they also contain trace toxic/hazardous heavy metals such as Cu, Zn, Pb, and As [1], which limit their usage in pig iron industry [2,3]. At present, almost all of these cinders are dumping as solid wastes except for using as additives in some iron plants and cement manufacturers [4]. The increasing dump not only occupies plenty of land, but also wastes iron resources. The most important problem is that it puts a serious threat to the environment due to water pollution.

Using pyrite cinders in iron oxide preparation is one of the promising ways for pyrite cinders reutilization because of the increasing demand for iron oxide pigments driven by the increasing consumption in industry. Moreover, iron oxide is characterized by non-toxicity, chemical stability, durability, variety of colors [5] and low costs [6]. Some papers have already reported the preparation of iron oxide from pyrite cinders by hydrometallurgy [7,8], which has attracted worldwide attention due to its advantages such as process simplicity, high efficiency, low pollution and easy-to-build equipments.

The preparation of iron oxide from pyrite cinders by hydrothermal method has been extensively investigated by our group [9,10]. It was found that Fe(II) played a very important role during the phase transformation from ferric hydroxide gel to hematite in a neutral medium, and Fe(II) also had a significant effect on hematite's morphology and size. The aim of this paper is 1) to investigate the effect of Fe(II) on the formation of iron oxide phases, 2) to examine the effect of Fe(II) on the properties of the prepared iron oxide, and 3) to propose a possible mechanism for hematite preparation with/without Fe(II).

2. Experimental

2.1. Materials

Reagent-grade H_2SO_4, H_2O_2 and $NH_3 \cdot H_2O$ (Tianjin Kaitong Chemical Co.) were used without further purification. Ultrafine iron oxide particles (Hunan Three Ring Pigment Co.), uniform in spherical shape, about 0.3 μm in diameter, were used as seed crystal. Pyrite cinders were provided by Guangdong Pyrite Mine Corporation, China. Its chemical composition was examined by X-ray fluorescence spectroscopy (XRF), and the results were presented in Table 1.

The mixture of ferric and ferrous sulfate (lixivium) was obtained by leaching pyrite cinders with sulfuric acid [11]. In details, 6.5 L 50 wt.% sulfuric acid solution was added to a three-necked flask (10 L in

---

* Corresponding author. Tel.: +86 731 88836258; fax: +86 731 88710171.
E-mail address: csuzzyyjj01@yahoo.com.cn (Y. Zheng).

doi:10.1016/j.powtec.2011.02.019

Table 1
Chemical composition (wt. %) of investigated pyrite cinders by XRF.

Components	wt.%	Components	wt.%
Fe	58.15	Ti	0.053
SiO_2	11.88	Ba	0.059
SO_3	4.88	Na	0.05
Al_2O_3	3.06	Zn	0.148
CaO	1.46	Cu	0.011
MgO	0.61	Cr	0.010
K_2O	0.52	P	0.011
MnO_2	0.27	Bi	0.010
PbO	0.19	Zr	0.004

volume). Then, 3 kg pyrite cinders were gradually added under vigorous stirring at 115 °C for 4 h. After filtration, the solution was diluted to 9.0 L with deionized water. The diluted solution, used as iron source for hematite preparation, was mainly a mixture of ferric sulfate and ferrous sulfate (Table 2), containing trace other elements such as Al, Mg, and Ca.

2.2. Experimental procedures

Iron oxide particles were prepared from pyrite cinders lixivium by hydrothermal process. The standard procedure was as follows. Hydrogen peroxide solution was dropped into the diluted solution (Section 2.1) under vigorous stirring, adjusting $n_{Fe(II)}/n_{Fe(III)}$ to a desired value. Ammonia solution (25 wt. %) was then added until pH reached 7. Subsequently, 2 g ultrafine hematite particles were added and the total volume was adjusted to 400 mL with deionized water. The obtained suspension was transferred to a 500 mL stainless steel autoclave. Then it was sealed, heated at 230 °C for 0.5 h. After that, the autoclave was cooled down to room temperature by an internal cooling coil. After filtration, the resulting products were rinsed with deionized water and dried at 105 °C for 12 h.

2.3. Analysis and characterization

The liquids and solids were analyzed to examine the ferrous and ferric ion concentration according to GB 1863-2008 (China industrial standard). Some typical products were digested and analyzed by Inductively Coupled Plasma Optical Emission Spectrometer (ICP-OES, OPTIMA 2000, PerkinElmer, USA). X-ray powder diffraction (XRD) analysis was conducted on a Rigaku D/max-TTR III X-ray diffractometer using CuKα radiation (λ = 1.54056 Å). Fourier transform infrared (FT-IR) spectra were recorded at RT using a Nicolet IS 10 infrared spectrometer in the region of 2000–500 cm^{-1}. Morphology and size of the products was characterized using a FEI Quanta 200 scanning electron microscope (SEM). Some typical products were also observed using a Hitachi Model H-800 transmission electron microscope (TEM).

3. Results and discussion

3.1. X-ray powder diffraction

Table 2
Chemical composition of the pyrite cinders lixivium.

Element	Content (g/L)	Element	Content (g/L)
Fe	163.74	P	0.135
S	162	K	0.11
Al	1.154	Si	0.023
Zn	0.312	Pb	0.067
Mn	0.314	Ti	0.038
Ca	0.327	Cu	0.013
Mg	0.355	Na	0.03

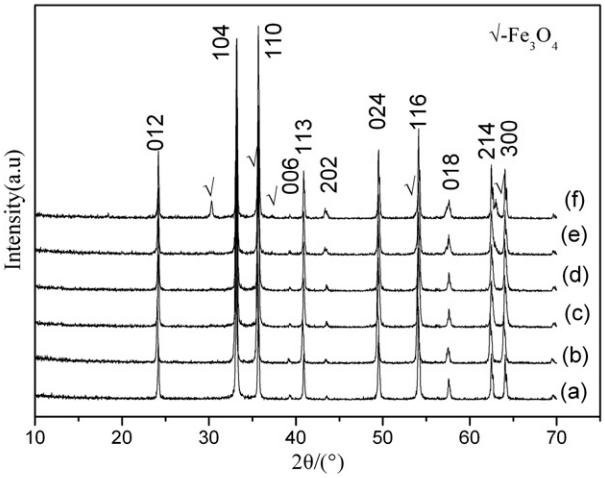

Fig. 1. XRD patterns of hydrothermal products synthesized at different $n_{Fe(II)}/n_{Fe(III)}$ ratio (a) $n_{Fe(II)}/n_{Fe(III)} = 0$, (b) $n_{Fe(II)}/n_{Fe(III)} = 0.04$, (c) $n_{Fe(II)}/n_{Fe(III)} = 0.07$, (d) $n_{Fe(II)}/n_{Fe(III)} = 0.08$, (e) $n_{Fe(II)}/n_{Fe(III)} = 0.1$, and (f) $n_{Fe(II)}/n_{Fe(III)} = 0.12$.

Fig. 1 showed the XRD patterns of the hydrothermal products obtained at different $n_{Fe(II)}/n_{Fe(III)}$ ratios. As observed, all the XRD spectra except Fig. 1(f) were in good agreement with that of the standard pattern for rhombohedra α-Fe_2O_3 (space group: R-3c (167), cell constants of which were a = b = 5.036 Å and c = 13.749 Å (JCPDS, No. 33-0664)). And these peaks were very intensive, indicating a high crystallinity. But both α-Fe_2O_3 and Fe_3O_4 were observed when $n_{Fe(II)}/n_{Fe(III)}$ was 0.12 (Fig. 1(f)). Thus, it was not easy to obtain a pure-phase product at a relatively high $n_{Fe(II)}/n_{Fe(III)}$ ratio, and pure α-Fe_2O_3 formation may be favored by low $n_{Fe(II)}/n_{Fe(III)}$ ratio.

Fe(II) content of the synthesized products at different $n_{Fe(II)}/n_{Fe(III)}$ ratios was determined to further understand the role of ferrous ions in the crystalline formation, and the results were shown in Fig. 2. From Fig. 2, it was found that when $n_{Fe(II)}/n_{Fe(III)}$ was lower than 0.1, with the increase of $n_{Fe(II)}/n_{Fe(III)}$, Fe(II) content of the synthesized products increased slowly, because Fe(II) ions may be adsorbed on the surface of α-Fe_2O_3 particles. Fe(II) content of the products obtained at $n_{Fe(II)}/n_{Fe(III)} > 0.1$ increased rapidly with the increase of $n_{Fe(II)}/n_{Fe(III)}$. The reason was that Fe(II) ions were incorporated to Fe_3O_4, which was consistent with the results of XRD analysis.

3.2. FT-IR spectroscopy

FT-IR spectra of hydrothermal products synthesized at different $n_{Fe(II)}/n_{Fe(III)}$ ratios were shown in Fig. 3. All the hydrothermal products showed

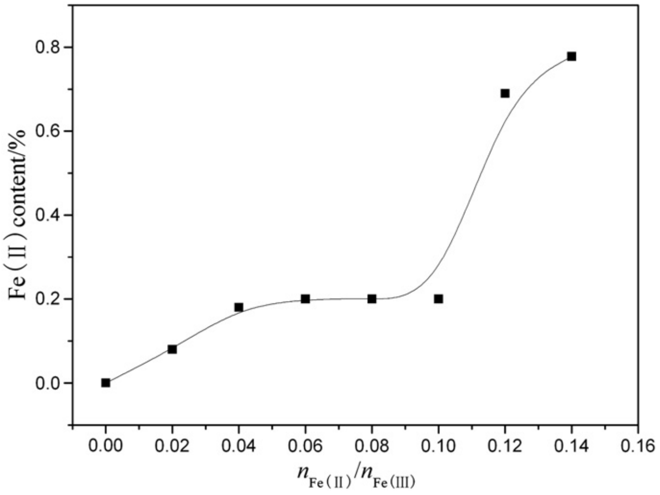

Fig. 2. Changes of Fe(II) content of hydrothermal products synthesized at different $n_{Fe(II)}/n_{Fe(III)}$ ratio.